Available online at www.sciencedirect.com
SCIENCE DIRECT®
Journal of Crystal Growth 269 (2004) 425–431
JOURNAL OF CRYSTAL GROWTH
www.elsevier.com/locate/jcrysgro

Growth and characterization of Zn–ZnO core-shell polygon prismatic nanocrystals on Si

Chin-Ching Lin, Kun-Ho Liu, San-Yuan Chen*

Department of Materials Science and Engineering, National Chiao-Tung University, 1001 Ta-hsueh Road, Hsinchu 300, Taiwan, Republic of China

Received 11 March 2004; accepted 14 May 2004

Available online 24 June 2004

Communicated by D.W. Shaw

Abstract

Zn precursor synthesized from $Zn(ClO_4)_2$ solution was used as nucleation seeds for the growth of Zn polygon prismatic nanocrystals on silicon via a thermal vapor transport at low temperatures of 150–400°C (substrate) in Ar atmosphere. Depending on different reaction temperature and atmosphere, Zn–ZnO core-shell polygon prismatic nanocrystals with a dimension from nanometer to micrometer can be developed as evidenced from high-resolution transmission electron microscopy and auger nanoprobe electron spectroscopy analysis. The Zn–ZnO polygon prismatic structure shows weak UV emission and strong deep-level emission. However, photoluminescence properties and crystallization of Zn–ZnO prismatic nanocrystals could be improved by suitable post-treatment.

PACS: 81.10.Aj; 64.70.Fx; 64.72.−y

Keywords: A1. Photoluminescence; B1. Nanocrystals; B1. Zn; B1. ZnO

1. Introduction

In the nanoscience, self-assembly is one of the most important ''bottom-up'' approaches to achieve operable nanostructure. Exploration of techniques for building self-assembled nanostructures at all length scales and understanding the growth mechanisms are essential for achieving superior functionality. Structures formed by self-assembly have been investigated for a wide range of metallic [1–3], semiconductor [4], and oxide [5] nanocrystals. In the pass few years, much effort has been invested in controlling the sizes and shapes of inorganic nanocrystals, because these parameters represent key elements that determine their physical properties [6,7]. Lee et al. [8] pointed out that the crystalline phase of the seeds at the nucleation stage is critical for directing the intrinsic shapes of nanocrystals due to its characteristic unit cell structure. Further delicate shape control is also possible through the nanocrystals during kinetically controlled growth process [9].

*Corresponding author. Tel.: +886-3-5731818; fax: +886-3-5725490.

E-mail address: sychen@cc.nctu.edu.tw (S.-Y. Chen).

0022-0248/$ - see front matter © 2004 Elsevier B.V. All rights reserved.
doi:10.1016/j.jcrysgro.2004.05.064

To date, extensive research work has been focused on ZnO, which is one of the most useful oxides for nanodevices such as photo-detector, [10] solar cells, [11,12] nanolasers, [13] and micro-cavities [14] because ZnO possesses unique optical and electrical properties such as a direct bandgap of 3.37 eV and large exciton binding energy of 60 meV. Owing to their promising use in optical and electronic devices, many different morphological ZnO nanostructures, including nanowires, [15] nanorod, [16] nanocables, [17] nanoribbons [18] and nanoblets [19] have been synthesized by various techniques.

Recently, Gao et al. reported a new structure with mesoporous polyhedral cages and shells formed by textured self-assembly of ZnO nanocrystals by a solid-vapor deposition process at a high temperature of 1150°C [20]. The formation process of the polyhedral ZnO shell and cage structures was proposed to be a process comprised of solidification of liquid droplets, surface oxidation, and sublimation. The growth mechanism may be used for the development and control of the crystal growth. However, no systematical study was reported for the self-assembly process of polyhedral Zn–ZnO crystals with a dimension from nanometer to micrometer at low temperatures. Therefore, we have combined the aforementioned vapor-gas with liquid-solution methods for growing Zn/ZnO polygon prismatic nanocrystals. The liquid-solution method supplies the uniform nanoseeds to serve as nuclei and the subsequent vapor-gas phase method provides the Zn source for the growth of nanocrystal Zn/ZnO. Herein, by varying different concentration of the heterogeneous nucleus sites and growth temperature range, we successfully control the structure size and morphology of self-assembled Zn and Zn–ZnO core-shell nanocrystals. Besides, a surface oxidation process was also applied to verify the stability of the structure.

2. Experimental procedure

Following the process proposed by Koch et al. Zn precursor was prepared in methanol with 50 ml of 10^{-2} M $Zn(ClO_4)_2$ solution with an addition of 442 ml methanol plus 8 ml 5 M NaOH and left for 24 h overnight [21]. Extremely small colloidal particles (<7 nm) are obtained in this solution. Subsequently, the Si substrate was coated with various concentrations of the colloid and then located downstream of the carrier gas flow in the alumina tube, where the tube was sealed and evacuated by a mechanical rotary pump to a pressure of 80 mTorr. In this study, ZnO and graphite powders were ball-mixed in ethanol for 15 h and then used as for the growth source of Zn nanocrystals. The source material was placed on an alumina boat and positioned at the center of the alumina tube. High-purity Ar was used as carrier gas with a flow rate of 10 s.c.c.m. to provide Zn source for the formation of Zn polygon prismatic nanocrystals at a substrate temperature of 150–400°C for 0.5–4 h. After that, the obtianed polyhedral structures were thermally annealed at 500°C in pure oxygen atmosphere (5 N) for 0.5–5 h to study the changes of morphology and crystallization.

The deposited polyhedral structures were observed by scanning electron microscopy (FE-SEM, S-4100), and the crystal structure was analyzed using XRD (Siemens D5000). The depth profile of ZnO–Zn polyhedral structure was measured using an AES (Auger Nanoprobe Electron Spectroscopy, Auger 670 PHI Xi). Transmission electron microscopy (TEM Philips TECNAI 20) attached with energy-dispersive X-ray spectroscopy (EDS) operated at 200 KeV was also used for nanostructural analysis. Photoluminescence (PL) measurement was performed by excitation from 325 nm He–Cd laser at room temperature.

3. Results and discussion

As the substrate coated with the precursor of Zn-colloid was placed in the alumina tube at 250°C for 30 min, as shown in Fig. 1(a), it was observed that the nanoparticles were not uniformly dispersed on the Si substrate that can be attributed to too small colloidal particles (much less than 10 nm in diameter) and high electrostatic force. With an increase of reaction time up to 1 h, the aggregated nanoparticles tend to form a

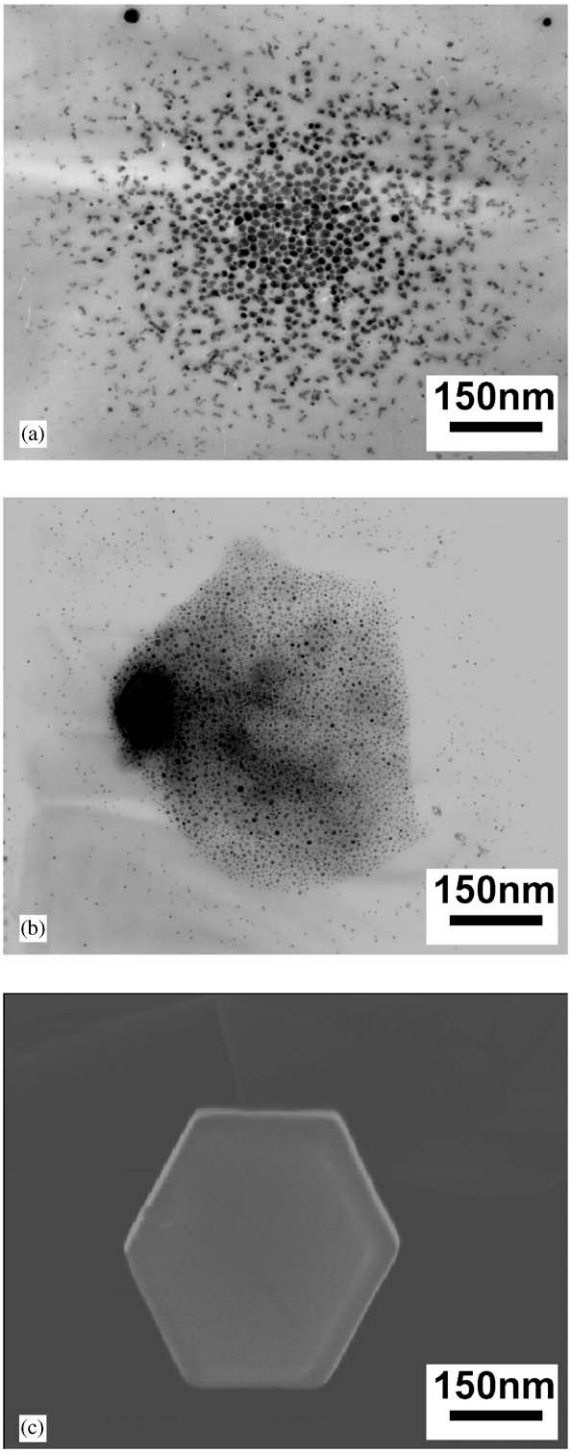

(0 0 0 1) hexagon-based shape composed of many small colloids as shown in Fig. 1(b) because of their highest surface energy. The spreading region composed of Zn nanocrystals has a diameter around ~250 nm. As the reaction time exceeds 2 h, it was found that the composing-crystals are grown into a polyhedral structure that is enclosed by (0 0 0 1), $\{1\,0\,\bar{1}\,0\}$, $\{1\,0\,\bar{1}\,1\}$, and high-index planes [10] Fig. 1(c). It suggests that the spatial distribution region of Zn nanocrystals would become a base for the development of larger-size polygon prismatic crystals. Based on the above argument, the relative colloidal concentration determines the agglomerate degree of nanoparticles. Hence, it is expectable that a higher colloidal concentration obtains a larger amount of agglomerate region and the size of the structure by self-assembly Zn nanocrystals is also bigger. The average size of these agglomerate polyhedral nanocrystals is estimated about 150–250 nm as shown in Fig. 2.

It is well known that metallic material becomes unstable when the temperature closes to its melting point and the apparent melting point (for Zn: 410°C) will be reduced for metallic crystals with significantly reduced size. The observation suggests the existing of critical condition depending on the competition between thermodynamics and kinetics. Above the critical period, a prolonged heat-treatment or higher-temperature causes the Zn nanocrystals to become structurally unstable in Ar atmosphere. However, it was detected that a thin oxide layer has been developed on the surface of the Zn polyhedron. Therefore, an oxidation treatment is applied to modify the surface status of Zn polygon prismatic crystals and to keep the stability of growing crystals because both Zn and ZnO have the same hexagonal (hcp) structure. From the viewpoint of growth kinetics, rearrange-

Fig. 1. Growth of Zn nanocrystals as a function of growth time at 250°C: (a) at 30 min, TEM image of the nuclei (<10 nm) for Zn polygon prismatic nanocrystals, (b) at 1 h, TEM image showing a special distribution pattern composed of Zn polygon prismatic nanocrystals formed by thermal vapor process, and (c) at 2 h, SEM image of Zn polygon prismatic crystals (~250 nm) developed from the clusters of the ultra-fine Zn nanocrystals.

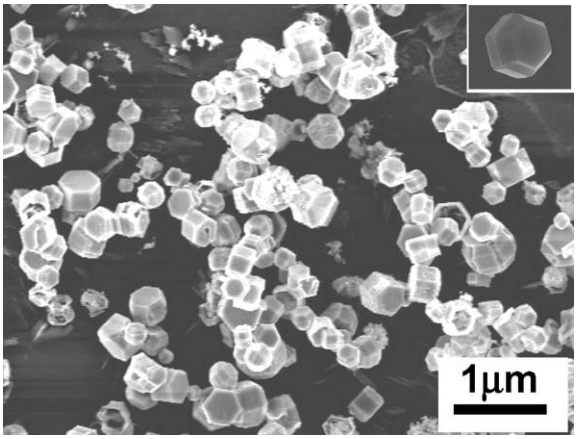

Fig. 2. SEM images of agglomerated polyhedral Zn nanocrystals synthesized by liquid solution and vapor transport method with average particle size of 150–250 nm in diameter.

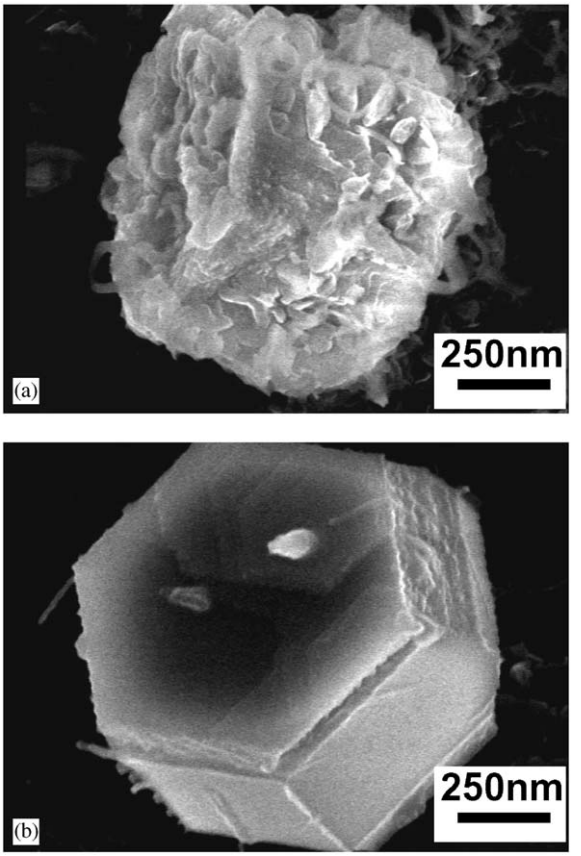

Fig. 3. SEM images of Zn polygon prismatic nanocrystals grown at 250°C in pure argon and then rapidly annealed at 500°C for 3 h (a) without and (b) with oxidation treatment.

ment of the sublattices of zinc from hcp (Zn) to hcp (ZnO) would occur on the surface of Zn nanocrystals following the Zn template. As shown in Fig. 3(a), after thermal treatment at 500°C for 3 h without oxygen supplied, the surface morphology of polyhedral structures becomes disintegrated. However, thermal-treatment at the same temperature in oxygen atmosphere could retain the complete polyhedral structures Fig. 3(b). It is attributed to the formation of ZnO layer on the surface of Zn polyhedral structures by oxygen treatment that probably prevents the crystals from disintegration. As evidenced from the X-ray diffraction (XRD) patterns in Fig. 4, the sample grown in pure argon at 250°C for 2 h shows only the crystalline phase of Zn element Fig. 4(a). However, for the Zn polyhedral structure subjected to oxidation treatment at 500°C, ZnO crystalline phase can be developed from Zn surface as identified from the XRD in Fig. 4(b). Chemical composition microanalysis by energy-dispersive spectrometry (EDS) reveals that the relative atomic ratio of Zn to O is about 15:1 for Zn polyhedral structures with oxidation treatment. This is in good agreement with the XRD analysis.

The growth mechanism of the novel polyhedral structure is illustrated in Fig. 5 that is different from the mechanism reported by Gao et al. [20] After the $Zn(ClO_4)_2$ solution containing Zn colloid was deposited on the Si substrate, the solvent begins to evaporate and droplets act as nucleation seeds. Then, these nuclei would cap these Zn molecules to develop the nanocrystals when Zn sources were transported by thermal evaporation process. Moreover, during thermal evaporation process, these nuclei become unstable. Zn nanocrystals would be assembled by attractive force to form a base of polygon prismatic crystals and organized in a compact hexagonal network. The "island growth" model can be introduced to explain our controlling mechanism. After the Zn colloids were deposited on the Si substrate, the introduced Zn vapor would be preferentially deposited at the heterogeneous sites that were provided by previous coated nanoparticles. Sub-

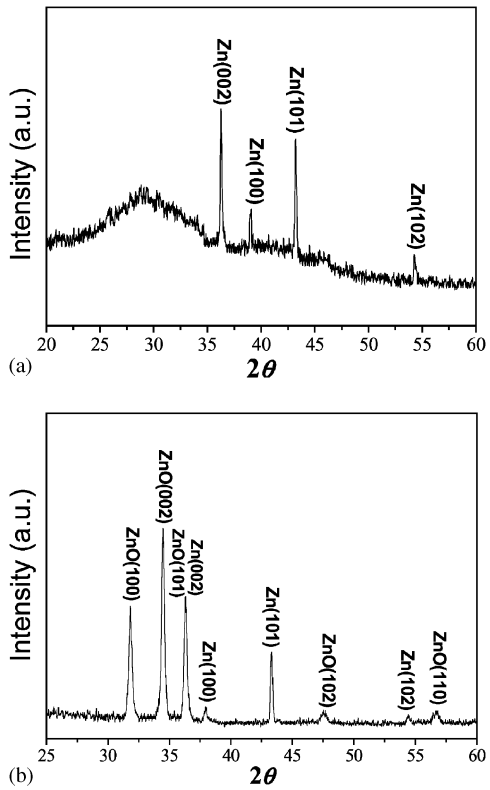

Fig. 4. XRD patterns of Zn polygon prismatic nanocrystals (a) grown at 250°C in pure argon and (b) then rapidly annealed at 500°C for 3 h in oxidation atmosphere.

sequently, these deposited atoms have a tendency to close together and form islands if atoms are more strongly bound to each other than to substrate. In a lower growth temperature and more concentration situation, stronger binding force between atoms and slower diffusion rate result in the Zn island formation. As the oxidation treatment is applied, the surface status of Zn polygon prismatic crystal is modified and rearrangement of the sublattices of zinc from hcp (Zn) to hcp (ZnO) would occur on the surface of Zn nanocrystals following the Zn template. Therefore, Zn–ZnO core-shell structure as well as crystalline ZnO nanomaterials would be formed. As shown in Fig. 6, the high resolution TEM of a Zn–ZnO core-shell crystal demonstrates that there exists a good epitazial relationship between Zn core and ZnO shell. The singular fringe spacing of the core material (Zn) was measured to be 0.24 nm, which agrees well with the (1 0 0) spacing of wurtzite-Zn, while the value of the shell material (ZnO) is about 0.28 nm, which agrees well with the (1 0 0) spacing of wurtzite-ZnO. In addition, a regular array of misfit dislocations (marked with arrows) is revealed at Zn/ZnO interface. These generated dislocations possibly serve to accommodate the relatively large lattice mismatch between Zn and ZnO (17%).

In order to further confirm the effect of oxidation on morphology and chemistry of ZnO–Zn polyhedral structures, the depth profile of Zn polyhedral structures with oxidation treatment was measured by auger nanoprobe electron spectroscopy (AES) where the Zn polyhedral crystal with 300–400 nm in length and ~250 nm in diameter was used for the AES analysis. For the sample Fig. 7(a) treated at 500°C in pure oxygen atmosphere for 2 h, the depth profile of Zn polyhedral structures in Fig. 7(b) illustrates that the signal of oxygen element is detected from surface to a depth of 100 nm from the surface region. It implies that Zn–ZnO core-shell nanostructure can be developed from Zn polyhedral structures with oxygen treatment.

The PL measurements of the synthesized Zn polyhedral structures were performed at room temperature, using a He–Cd laser line of 325 nm as the excitation source. As shown in Fig. 8, UV and green emission with peaks at 378 and 530 nm are observed for the Zn polyhedral structures with oxidation treatment that is different from that of Zn polyhedral structures without oxidation treatment, where no emission peak was found because of only pure metal Zn in this case. On the contrary, as the Zn polyhedral structures were subjected to oxidation treatment, the surface would form an oxide layer. According to XRD analysis, the oxide layer is basically zinc oxide. ZnO usually displays two major PL peaks, UV (near-band-edge) emission peak and green (or red) emission peak (deep-level). The deep-level emissions are generally associated with defects in ZnO lattice such as oxygen vacancies (V_o) and Zn interstitials (Zn_i). Although the developed Zn polygon prismatic nanocrystals are well crystalline, a large lattice mismatch (17%) can be induced in the interface of

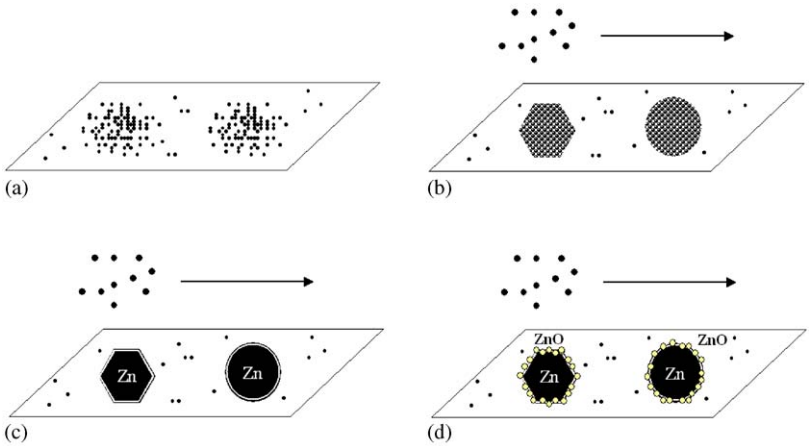

Fig. 5. Schematic illustration for the growth mechanism of Zn/ZnO polygon prismatic nanocrystals.

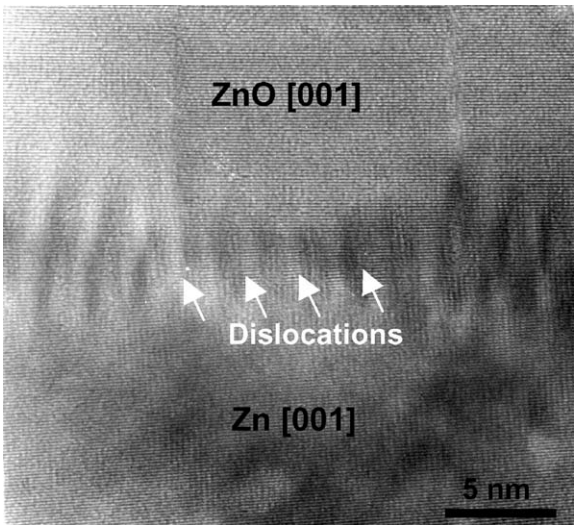

Fig. 6. High-resolution TEM image of the heterostructure of the Zn/ZnO core-shell nanocrystals.

Zn and ZnO that becomes the defect generator and causes the strong deep-level emissions, in contrast to that of pure ZnO. In addition to lattice mismatch, an incomplete oxidation of zinc produces some defects inside surface layer and gives deep-level emission, too. However, with an increase of the thickness of oxide layer, the peak intensity of deep-level emission is reduced but the UV emission is enhanced. It indicates that the UV emission can be improved by controlling the oxidation in Zn polyhedral structures.

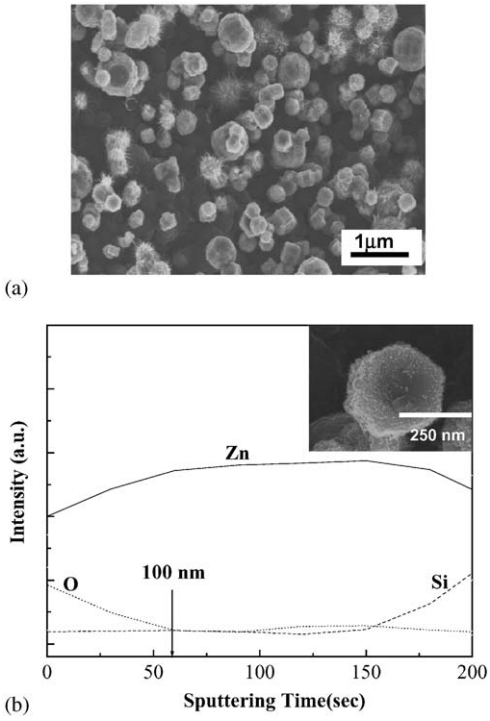

Fig. 7. (a) Oxygen-annealed Zn polygon prismatic nanocrystals and (b) depth profiles of Zn polygon prismatic nanocrystals, demonstrating the formation of Zn–ZnO core-shell structure.

4. Conclusions

Zn polygon prismatic nanocrystals are synthesized by liquid-solution seed nucleation and vapor-

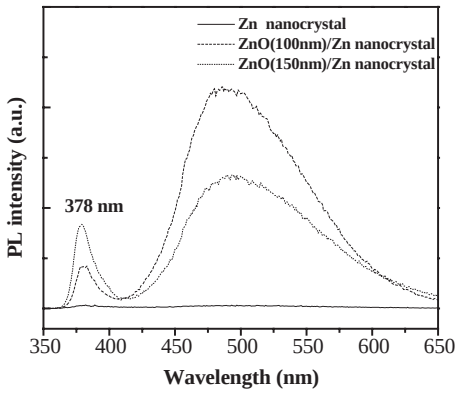

Fig. 8. Room-temperature photoluminescence spectra recorded from Zn polygon prismatic nanocrystals without and with (500°C for 2 and 4 h) oxidation treatment.

gas growth method. The dimension of Zn crystals can be controlled depending on treatment temperature and $Zn(ClO_4)_2$ concentration in the liquid solution. After oxidation treatment, the ZnO surface layer can be developed on the Zn nanocrystals to form Zn–ZnO core-shell structure and remain stable at higher temperatures. Moreover, the thickness of oxide layer in Zn–ZnO polygon prismatic nanocrystals can be effectively controlled and the PL properties of Zn–ZnO nanocrystals can be improved by oxidizing the Zn nanocrystals to form ZnO. These formed Zn–ZnO nanocrystals can be further used as building blocks to assemble two- or three-dimensional photonic crystals.

Acknowledgements

The authors gratefully acknowledge the National Science Council of the Republic of China for its financial support under Contract No. NSC-92-2216-E-009-014.

References

[1] S.H. Sun, C.B. Hurray, D. Weller, Li. Folks, A. Moser, Science 287 (2000) 1989.
[2] M.P. Pileni, J. Phys. Chem. B 105 (2001) 3358.
[3] C.J. Kiely, J. Fink, M. Brust, D. Bethell, D. Schiffrin, Nature 396 (1998) 444.
[4] S.G. Peng, L. Manna, W.D. Yong, J. Wickham, E. Scher, A. Kadavanich, A.P. Alivisatos, Nature 404 (2000) 59.
[5] J.S. Yin, Z.L. Wang, Phys. Rev. Lett. 79 (1997) 2570.
[6] L.M. Lieber, Solid State Commum. 107 (1998) 607.
[7] A.P. Alivisatos, Science 271 (1996) 933.
[8] Z.A. Peng, X.G. Peng, J. Am. Chem. Soc. 123 (2001) 1389.
[9] X. Peng, Adv. Mater. 15 (2003) 459.
[10] J.A. Rodriguez, T. Jirsak, J. Dvorak, S. Sambasivan, D.J. Fischer, Phys. Chem. B 104 (2000) 319.
[11] K. Hara, et al., Sol. Energy Mater. Sol. Cells 64 (2000) 115.
[12] H. Rensmo, K. Keis, H. Lindstrom, S. Sodergren, A. Solbrand, A. Hagfeldt, S.E. Lindquist, L.N. Wang, M. Muhammed, J. Phys. Chem. B 101 (1997) 2598.
[13] M.H. Huang, S. Mao, H. Feick, Y.Y. Yan, H. Kind, E. Weber, R. Russo, P.D. Yang, Science 292 (2001) 1897.
[14] H.-J. Muhr, F. Krumeich, U.P. Schonholzer, F. Bieri, M. Niederberger, L.J. Gauckler, R. Nesper, Adv. Mater. 12 (2000) 231.
[15] Y.C. Kong, D.P. Yu, B. Zhang, W. Fang, S.Q. Feng, Appl. Phys. Lett. 78 (2001) 407.
[16] W.I. Park, Y.H. Jun, S.W. Jung, G.C. Yi, Appl. Phys. Lett. 82 (2003) 964.
[17] Y. Zhang, K. Suenaga, C. Collies, S. Iijima, Science 281 (1998) 973.
[18] W. Shi, H. Peng, N. Wang, C.P. Li, L. Xu, C.S. Lee, R. Kalish, S.T. Lee, J. Am. Chem. Soc. 123 (2001) 11095.
[19] Z.W. Pan, Z.R. Dai, Z.L. Wang, Science 291 (2001) 1947.
[20] P.X. Gao, Z.L. Wang, J. Am. Chem. Soc. 125 (2003) 11299.
[21] U. Koch, A. Fojtik, H. Weller, A. Henglein, Chem. Phys. Lett. 122 (1985) 507.